Temperature Determination in Optoelectronic Waveguide Modulators

M. Allard, R. A. Masut, and M. Boudreau

***Abstract*—Optoelectronic devices are particularly sensitive to temperature changes induced by the absorption of light and the passage of current. In order to study the thermal issues arising in a InGaAsP-based Mach–Zehnder (MZ) optical modulator, a nonlinear finite-element thermal model of the device was constructed. The model considers the variation with temperature of both the thermal conductivity of the semiconductors composing the device and the optical absorption. To that effect, the optical absorption was measured inside the waveguide as a function of temperature. An experimental method using liquid crystals to measure the surface temperature was also developed. Both were used to evaluate the temperature inside a variable optical attenuator present on the modulator. Good agreement with the model and the experiment is found over a wide range of operating conditions. These tools are expected to play a key role in understanding thermal issues in future photonic devices, in view of the desire to integrate multiple devices on a common substrate and the continuous increase of the optical powers in fiber systems.**

***Index Terms*—Liquid crystals, optical modulator, optoelectronics, temperature measurements, thermal model.**

I. Introduction

OPTOELECTRONIC components are particularly sensitive to the temperature distribution within the active region of the device, since many material properties, such as the band gap and the refractive index, vary with temperature. Internal heating is frequently observed in these devices and is usually the consequence of current flow or of the absorption of light. Heating can have several important and potentially detrimental effects on the operation and the reliability of optoelectronic devices. For example, an increase in the internal temperature may affect the wavelength of emission of a laser diode or the switching voltage of an optical modulator, or accelerate degradation processes in any device. Thermal issues are especially important in reliability testing, where devices are usually submitted to high stress conditions, typically involving high temperatures, for extended periods of time.

Manuscript received June 2, 1999; revised January 28, 2000. This work was supported in part by the National Science and Engineering Research Council of Canada (NSERC).

M. Allard is with the École Polytechnique de Montréal–Département de génie physique et de génie des matériaux, Groupe de recherche en physique et technologie des couches minces, Succ. "Centre-ville," Montréal, PQ H3C 3A7, Canada. He is also with the Department of Electrical and Computer Engineering, University of Toronto, Toronto, ON M5S 3G4, Canada.

A. Masut is with the École Polytechnique de Montréal–Département de génie physique et de génie des matériaux, Groupe de recherche en physique et technologie des couches minces, Succ. "Centre-ville," Montréal, PQ H3C 3A7, Canada.

M. Boudreau is with the Optoelectronic Reliability Department, Advanced Technology Laboratory, Nortel Networks, Nepean K1Y 4H7, Canada.

Publisher Item Identifier S 0733-8724(00)05073-8.

Most of the work presented in this article has been carried out on the Mach–Zehnder (MZ) optical modulator fabricated by Nortel Networks and used in high-speed transmitter modules for optical fiber telecommunications. Despite the importance of temperature in this device, there exists no simple way of measuring the internal temperature, so it is necessary to develop new experimental and theoretical tools to obtain this information. In this article, a thermal model of the optical modulator is presented [1]; the model was used to investigate thermal issues in the device and, more specifically, to study how the internal temperature depends on the operating conditions (applied voltage, photocurrent and optical power). The absorption coefficient in the waveguide, which depends on both the voltage and the local temperature, was measured and used in the model. An experimental technique was also developed, which uses liquid crystals to measure the temperature on the surface of the chip. This technique was used notably to validate the model predictions. The model and the experimental technique, used in conjunction, give an accurate understanding of the thermal properties of this device.

This paper first summarizes the operation of the MZ modulator. Many other methods of measuring the temperature of semiconductor devices exist and are briefly reviewed here; unfortunately, there are important limitations to their use in this case. The thermal model and the liquid-crystal technique are then described, following which the model predictions and the experimental measurements are presented and compared. The analysis has revealed specific thermal phenomena in the modulator, which are also discussed.

II. Description of the Optical Modulator

Optical modulators are used in high-capacity long-haul optical-fiber links where it is desirable to employ separate devices for light emission and modulation. This configuration solves the problem of the laser chirp, that is, the excursion of the emission wavelength when the laser current is modulated. The optical modulator, shown in Fig. 1, possesses two distinct sections: the modulator itself, described in reference [2], and an optical attenuator. Whereas the former accomplishes high-speed modulation of the optical signal, the latter provides variable dc attenuation to control the peak optical power exiting the device. The operating wavelength is 1.56 μm. The device is composed of a ridge waveguide defined on an InP substrate; in the modulator, the waveguide splits into two branches, which recombine after a certain distance to form an MZ interferometer. The waveguide comprises the active layer composed of multiple InGaAsP quantum wells, and is covered by a gold electrode. The quantum well

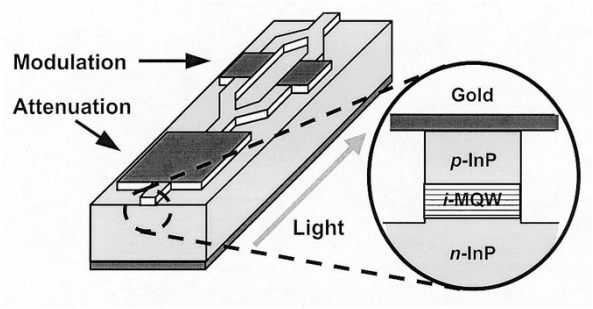

Fig. 1. The MZ optical modulator. Not all semiconductor layers are shown.

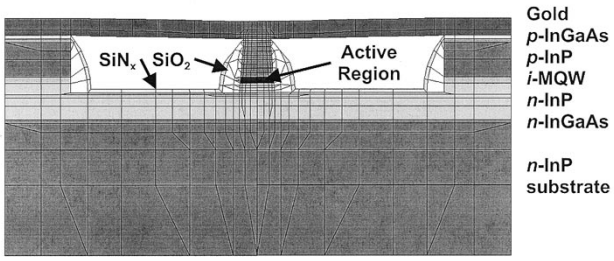

Fig. 2. An enlarged view of the ridge area, under the attenuation pad. The gold pad is seen on top, forming an air bridge over the hollow regions shown as white areas. The mesh shown is actually used in breaking up the structure in finite elements.

structure is identical in all sections of the device. The p-n junction formed in the waveguide can be reverse-biased in either arm by applying a negative voltage to the top electrode with respect to the substrate electrode; this modifies the effective refractive index in the waveguide, because of the quantum-confined Stark effect. Changing the voltage applied to the electrode covering each arm modifies the interference condition, and fast intensity modulation can be achieved with rapid voltage switching.

The operating voltage of the modulator is chosen so that little absorption occurs in the waveguide. In contrast, the voltage applied to the attenuator is typically higher by a few volts, which causes significant absorption in the waveguide, due again to the quantum-confined Stark effect. Controllable attenuation is achieved by adjusting the voltage. The electrode covering the attenuator is a large square gold pad, 220-μm-long, designed to efficiently dissipate the heat produced when the photocurrent, generated when light is absorbed, flows across the quantum wells. Since the highest temperature rise is expected to be found in the attenuator, most of the modeling efforts and experimental measurements have been devoted to this device.

At this point, it is important to note that two types of devices were investigated, the first being simple stand-alone modulators. In the second type of device, a laser diode has been attached to the modulator to form an integrated laser-modulator. The waveguide is continuous in both devices, and the distance separating the laser top-side electrode and the attenuator electrode is 80 μm. The heat produced in the laser section is expected to influence significantly the temperature distribution within the integrated device.

III. Methods of Evaluation of Temperature

Temperature influences the behavior of semiconductor devices, and many sophisticated methods have been developed for measuring the temperature in these devices. Infrared microscopy has been frequently used, mainly for microelectronic circuits [3], [4], while optical methods, such as photoluminescence, thermoreflectance and Raman spectroscopy, are well suited to measure temperature in optoelectronic devices, such as laser diodes [5]–[7]. Unfortunately, these conventional techniques are of very limited use on the optical modulator. The spatial resolution of infrared microscopy (5–10 μm) is not sufficient to probe the 2-μm-wide ridge of the MZ modulator, and the presence of a gold pad covering the region of interest of the waveguide forbids the use of methods employing an optical probe signal to measure the temperature of semiconductors.

On the other hand, the liquid-crystal technique described in this paper does not suffer from such limitations. However, it can only measure the temperature on the surface of the device, whereas the most valuable information is the temperature in the active region. Because the metallic pad efficiently dissipates the heat generated in the active region once it reaches the device surface, the surface and internal temperature can differ significantly. One efficient way of determining the temperature in the active region of the device is to construct a thermal model of the modulator.

IV. Thermal Model of the Attenuator Pad

The thermal model has been constructed with the aid of *Algor* [8], a commercial software package that uses finite-element algorithms to compute a three-dimensional temperature profile in the device. The model includes every semiconductor, dielectric, metallic and solder layer found in the actual device. Fig. 2 shows an enlarged view of the ridge area of the cross section of the model, clearly identifying each material. Note that only one half of the device is actually modeled, because it is symmetrical with respect to the vertical plane comprising the waveguide. Two versions of the model exist: one is the stand-alone modulator and the other is the integrated laser-modulator, which takes into consideration the effect of the laser heating. Although finite-element models are fairly common, the originality of this thermal model is that it takes into account the temperature dependence of both the thermal conductivity and the optical absorption in the waveguide, and is thus inherently nonlinear.

Heat is generated in the active region of the modulator when a photocurrent, resulting from the absorption of light, flows perpendicular to the quantum wells, and is extracted by a heat sink located directly under the n-side (bottom) electrode The contribution of the heat produced by the thermalization of the carriers after the photogeneration is negligible, since, at 1.56 μm, the excess of energy of the photons energy over the band gap is insignificant when compared to the energy conferred to the carriers by the external electric field. The heat is not generated uniformly along the length of the waveguide: how much heat is produced at one point along the waveguide is determined by how much light reaches that location and what the absorption coefficient is at that point. The situation is complicated by the fact that the absorption coefficient varies with temperature (as explained in the next section). To account for this, the waveguide is divided into many cells along the length of the waveguide, each

having the length of one element of the model; the absorption coefficient in each cell is at first determined from an initial uniform temperature. It is then a straight-forward task to compute how much light is absorbed in each cell and how much heat is produced. These data are then fed into *Algor*, which uses it to compute a temperature distribution in the device. In each cell, the temperature found in the active region is used to correct the initial guess for the absorption coefficient. The process is repeated in that manner until a self-consistent solution is reached; typically, 5–10 iterations are required.

Another unique aspect of this model is that it takes into consideration the temperature dependence of the thermal conductivity of the semiconductor materials, $\sigma(T)$. The latter is usually proportional to T^{-n} for the temperature range considered (20–250 °C); T is the absolute temperature and n is an exponent ranging between 1.2–1.5 [9]–[11], depending on the exact composition of the semiconductor. Because temperatures up to 250 °C are expected in the model, this dependence can not be overlooked. Although it is possible for the software to consider a conductivity that varies with temperature, the temperature transformation technique first used by Kirchoff was found to be more rapid and efficient [14]. It requires the use of an auxiliary variable, the transformed temperature, θ, defined as

$$\theta = T + \frac{1}{\sigma_0} \int_{T_0}^{T} \sigma(T)\, dT \tag{1}$$

where σ_0 is the thermal conductivity at any chosen reference temperature T_0. The interest of this technique is that a transformed temperature profile $\theta(x, y, z)$ can then be computed using a constant conductivity σ_0, and later on converted back to absolute temperature with the reciprocal transformation. The technique requires making the approximation that all materials composing the device can be described by the same exponent n. A value of $n = 1.4$ was used, since it lies between the exponent measured for InP ($n = 1.5$) [10] and the value suggested by Adachi for the InGaAsP composing the active region ($n = 1.375$) [11]. The largest error on the thermal conductivity of any material induced by this assumption is always less than 3% in the temperature range considered, which is judged acceptable.

The primary input parameters of the model are the voltage applied to the attenuator and the optical power delivered to the device. The model also requires the heat sink temperature, the optical absorption in the waveguide (described in the next section) and the thermal conductivity of all materials composing the device. The thermal conductivities have been obtained from the literature [12], [13]. Once all these secondary parameters are set, any given combination of voltage and optical power determine a unique photocurrent, which is a more convenient variable than the input optical power as it can be readily measured. It is very instructive to study the influence of voltage and photocurrent on the peak temperature found in the attenuator; thus, the model was run under various combinations of voltage and photocurrent, in order to produce temperature maps in the voltage-current plane. Once a maximum internal temperature is established to ensure the safe operation of the device, such maps can help to determine what operating conditions are safe or potentially harmful to the device.

V. Absorption Measurements

The temperature dependence of the effective absorption coefficient in the waveguide is a fundamental part of the thermal model. The dependence is a consequence of the fact that the semiconductor band gap varies with temperature. The method employed for these measurements is to inject light of limited power (to avoid internal heating) in the attenuator and to measure the photocurrent and optical power of the beam at the exit of the device, for every combination of voltage and stage temperature possible. The photocurrent is taken as being the total current flowing in the device, as the dark current was measured and found to be negligible. Fibers that had their end ground to form a taper (which acts like a lens) are used to couple light in and out of the waveguide. Tapered fibers are brought to a few microns from the waveguide facet and are more easily aligned than bulky lenses.

The absorption coefficient is retrieved from the measurements in the following manner. We first assume a unity quantum efficiency, that is, every absorbed photon generates one hole-electron pair that contributes to the photocurrent. The output coupling efficiency, η_{out} can be calculated by looking at the ratio of change of the photocurrent I and the output power L_{out} as voltage is increased, using the following equation:

$$\eta_{\text{out}} = \frac{-\Delta L_{\text{out}}}{\Delta I} \frac{e\lambda}{hc}. \tag{2}$$

The difference is taken between measurements at any pair of values of the voltage. The total optical power injected into the waveguide is calculated as

$$L_{\text{in}} = I \frac{hc}{e\lambda} + L_{\text{out}} \frac{1}{\eta_{\text{out}}}. \tag{3}$$

The light inside the waveguide does not depend on voltage and temperature. This approach allows us to disregard the input coupling loss.

The absorption coefficient was measured in the waveguide at temperatures ranging from 10 to 220 °C and at voltages from 0 to 10 V and the results are illustrated in Fig. 3. The absorption depends strongly on temperature, especially between 100–200 °C. At low and moderate temperatures, absorption increases rapidly with voltage, as expected, whereas the absorption becomes less dependent on voltage at high temperatures.

VI. Liquid-Crystal Technique

In a series of experiments, the liquid-crystal technique has proved to be an efficient tool for measuring the temperature on the surface of the device, and was used to assess the validity of the thermal model described in this article. This technique uses the transition between the nematic and isotropic phases of a liquid crystal, which occurs at a known temperature [15], [16]. In the nematic phase, all molecules are oriented along a common axis, and the liquid crystal exhibits birefringence, whereas it has no such property in its isotropic, true-liquid form. The transition

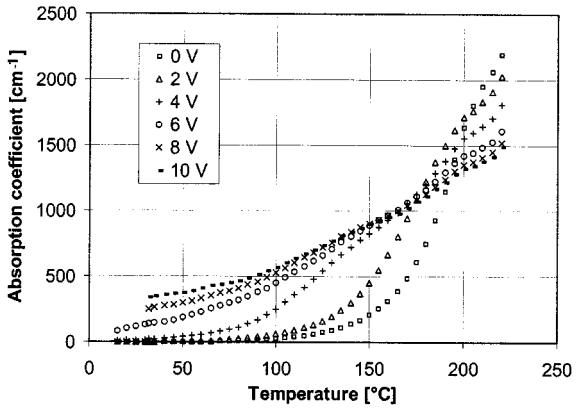

Fig. 3. Absorption in the waveguide as a function of voltage and temperature.

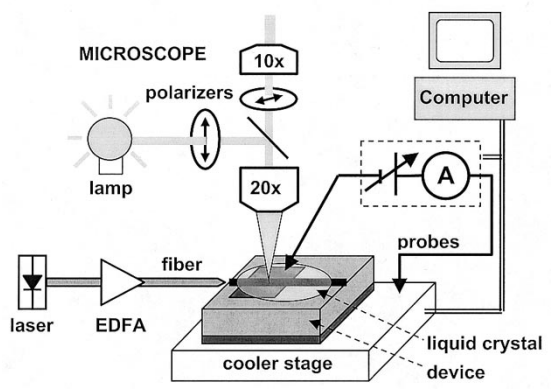

Fig. 4. Schematic view of the setup used for liquid-crystal temperature measurements.

can be observed with a microscope containing two crossed polarizing filters; a schematic view of the setup is shown in Fig. 4.

A hook-shaped probe tip attached to a micropositioner is used to deposit a droplet of liquid crystal onto the device surface. The sample is then heated past the transition temperature, where the liquid crystal is less viscous and forms a thin uniform film. This approach ensures that the liquid crystal remains on the device top surface and stays clear of the waveguide facets and avoids the difficulties of using chemical wetting agents [3]. The thin film of liquid crystal has a thickness not exceeding 5 μm, as verified with a high-resolution optical microscope.

The device, covered with liquid crystal, rests on a holder whose temperature is stabilized at 30 °C. The electrode is contacted with an electrical probe and biased while laser light is injected into the waveguide via a tapered fiber. In the case of the integrated laser-modulator, there is no need for an external light source. The device appears bright on a dark background in the microscope, since the birefringent liquid crystal modifies the state of polarization of the light, which can then be transmitted through the second polarizing filter. Where locally the temperature exceeds the transition temperature, a dark spot is observed, as light polarization is unchanged by the isotropic liquid crystal in these regions. The voltage is kept constant while the optical power in the waveguide is adjusted so that the dark spot is reduced to a minimal size; under these conditions, the peak temperature on the device surface is known to be the transition temperature.

(a)

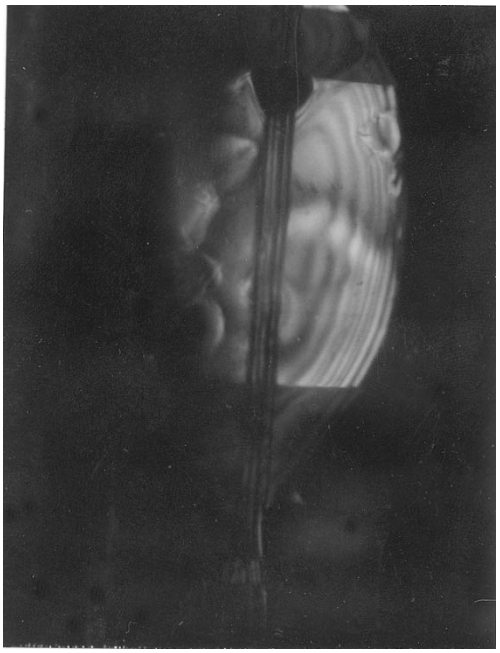

(b)

Fig. 5. The measurements of the surface temperature using liquid crystals. In (a), no external voltage is applied, while in (b), the device is biased and light is injected in the waveguide. The hot (dark) spot can be seen near the top edge of the pad. The ridge is in the center of the structure crossing the pad from top to bottom; the pad is 220 μm long.

Three different liquid-crystal mixtures were used (fabricated by Merck, Germany), with transition temperatures of 42, 58, and 73 °C (designated K21, E7, and N4, respectively), to extend the accessible temperature range. Fig. 5 shows a photograph of the attenuator pad covered with liquid crystal; a dark spot can clearly be seen at the top edge of the pad where the light

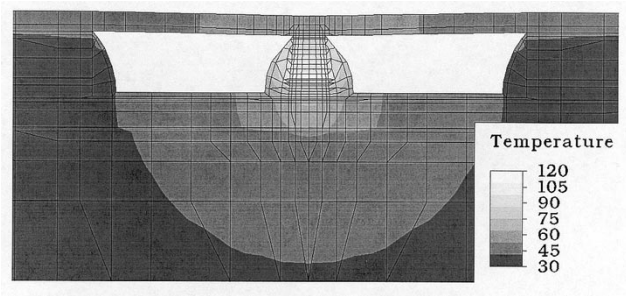

Fig. 6. Temperature profile in the cross-section of the device. The temperature (in degrees Celsius) is represented by a grey-scale, white being the hottest. This profile is taken at the front edge of the attenuator with a voltage of 8 V and a photocurrent of 10 mA.

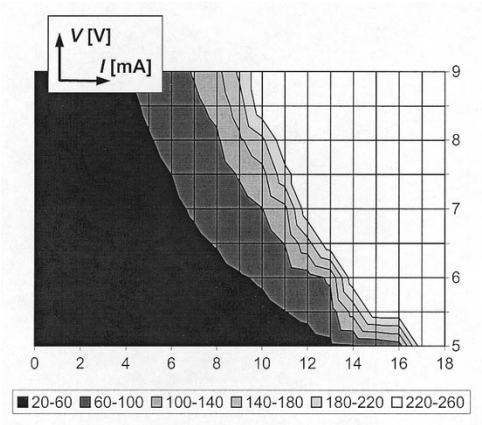

Fig. 7. Peak temperature in active region under the attenuator pad, as a function of voltage and photocurrent, in the stand-alone modulator. Isothermic line spacing is 40 °C. The absorption measurements were limited to 220 °C, so this is the maximum temperature predicted accurately by the model. The peak temperature was computed at integer values of the photocurrent (0, 1, . . ., 17 mA) and half-integer values of the voltage (5, 5.5, . . ., 9.0 V). The jagged nature of the isotherms comes from the interpolation scheme used by the plotting software.

enters. The highest optical power is found at this point, which corresponds to the point of highest temperature.

The liquid-crystal technique presents several interesting advantages over similar methods. It is inexpensive, nondestructive and does not require any elaborate sample preparation; it is also very versatile and can be used on other optoelectronic components such as laser diodes. The spatial resolution of this technique is the microscope optical resolution, approximately 1 μm. Once the transition in the liquid crystal is identified, the temperature on the chip surface is estimated to be within 1 °C of the nominal transition temperature, considering how precisely the transition temperature is known and how accurately the transition in the liquid crystal can be observed.

VII. Results and Discussion

Fig. 6 shows a typical modeled temperature profile in the cross section of the modulator in the attenuator; the temperature increase is confined inside the ridge, where all the heat is generated. Fig. 7 summarizes the results of the modeling work: it shows the peak temperature found in the active region under the attenuator pad in an integrated laser-modulator for different combinations of voltage and photocurrent, in the form of a temperature map. When high photocurrents are reached, the temperature increases very rapidly up to 220 °C, after which no absorption data is available. The rapid increase of temperature with photocurrent and voltage is explained by the fact that, as temperature rises to high levels, the absorption coefficient also increases rapidly, causing all the light to be absorbed within a short length of the waveguide. The heat is then generated in a smaller volume, increasing further the local temperature. This effect manifests itself as closely spaced isothermic lines in Fig. 7 at high photocurrents. To better understand this graph, note that at high voltages (above 6 V), almost all the light is absorbed over the length of the attenuator, so that, at a wavelength of 1.56 μm, an optical power of 10.0 mW in the waveguide (not in the fiber) corresponds to a photocurrent of 12.5 mA, assuming a unity quantum efficiency.

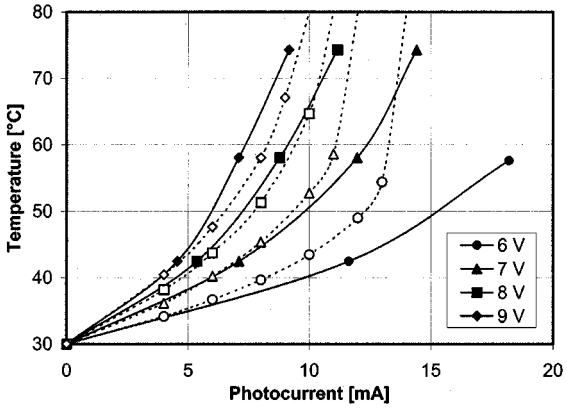

Fig. 8. Peak temperature on the surface of the attenuator pad in a stand-alone modulator. Both the liquid-crystal measurements (solid curves) and the model predictions (dotted curves) are illustrated for comparison. The lines joining the data points are only a guide to the eye.

The results of the liquid-crystal measurements are compared to the model predictions in Fig. 8. The different curves give the peak temperature found in the attenuator of the stand-alone modulator as a function of photocurrent, for discrete values of the voltage. No fitting of the model parameters has been performed to improve the agreement between modeling and experiment. The liquid-crystal measurements and the model predictions for the surface temperature are in good agreement, except for large values of the temperature ($T_{\mathrm{surf.}} > 60°$). This is believed to be due to the finite dimensions of the elements composing the model: under high temperature and consequently very high absorption conditions, all the absorption of the light occurs over a very short length of the waveguide, corresponding only to a small number of waveguide cells. The discrete nature of the finite-element model could then result in erroneous predictions. To verify this assertion, the dimension of the cells of the model was modified. It was found that the peak predicted temperature becomes dependent of the exact dimension of the cells in high photocurrent and temperature conditions. The finite-element thermal model is thus quantitatively accurate only up to moderate temperatures, where it is insensitive to the exact element dimensions. The model and the liquid-crystal technique were used on both stand-alone modulators and integrated laser-modulators, to investigate the effect of the heat generated by the laser diode on the temperature in the attenuator.

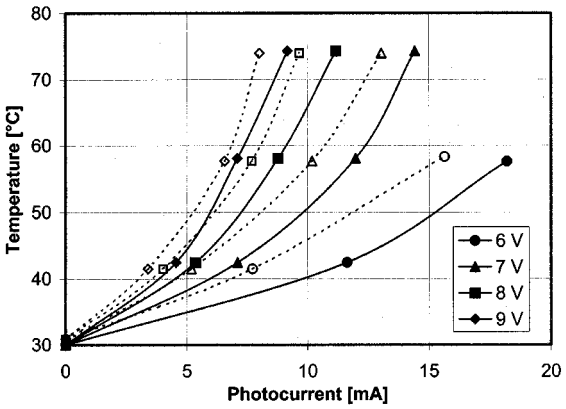

Fig. 9. Peak temperatures measured with the liquid-crystal technique on the surface of attenuator pads in integrated and stand-alone modulators, illustrating thermal crosstalk in the integrated device.

The peak surface temperature measured with the liquid crystal technique on both stand-alone and integrated devices is shown on Fig. 9, for various combinations of photocurrent and voltage. At all voltages, the maximum temperature measured on the pad is significantly higher in the integrated device. Although the results are not shown, the same conclusion can be reached from the modeling results. This is explained by direct conduction of heat from the laser to the modulator, which raises the modulator internal temperature. This effect is also multiplied, as the optical absorption in the waveguide then increases as a result of the temperature rise. Thus, this constitutes a direct evidence of thermal crosstalk in an integrated optoelectronic device, where the heat produced in one component of the device affects other neighboring components.

VIII. Conclusion

The importance of thermal issues in optoelectronic devices has been stressed in this article. Thermal issues arising in an optical MZ modulator were investigated with an experimental technique using liquid crystals to measure the surface temperature and an elaborate thermal model of the device. The experimental technique provided an efficient way of validating the model predictions, which accurately calculated the temperature in the modulator under a wide range of operating conditions. The model and the technique also successfully demonstrated that thermal crosstalk exists in integrated devices combining a laser and a modulator. The data obtained from this work has immediate uses in assessing what is the acceptable range of operating conditions of the attenuator based on the accelerated degradation occurring at high internal temperatures. Although the focus of this investigation was an optical modulator, the model and the liquid crystal technique can be readily adapted to study other waveguide devices such as laser diodes.

Thermal management is now becoming more important because of the ever-increasing optical powers used in optical telecommunications systems and the integration of several devices on a common substrate. Concurrently, new advanced components are presently being developed, such as optical switches, laser arrays, etc., where thermal issues similar to the ones described in this article could also arise. In this context, the availability of techniques for temperature measurements and thermal modeling is essential.

Acknowledgment

The authors would like to thank A. D. Smith, R. Greer, J. Yu, and R. Mallard for their contribution to this work.

References

[1] M. Allard, M. Boudreau, and R. A. Masut, "Thermal modeling and temperature measurements in optoelectronic waveguide devices," in *Proc. ICAPT'98, SPIE*, vol. 3491, Dec. 1998, pp. 478–481.

[2] C. Rolland, R. Moore, F. Shepard, and G. Hiller, "10 Gbit/s, 1.56 μm multiquantum well InP/InGaAsP Mach–Zehnder optical modulator," *Electron. Lett.*, vol. 29, no. 5, pp. 471–472, Mar. 4, 1993.

[3] M. Nishiguchi, M. Fujihara, A. Miki, and H. Nishizawa, "Precision comparison of surface temperature for GaAs IC's," *IEEE Trans. Comp., Hybrids, Manufact. Technol.*, vol. 16, pp. 543–549, Aug. 1993.

[4] M. Ashauer, J. Ende, H. Glosh, H. Haffner, and K. Hiltmann, "Thermal characterization of microsystems by means of high-resolution thermography," *Microelectron. J.*, vol. 28, no. 3, pp. 327–335, Mar. 1997.

[5] P. W. Epperlein, G. L. Bona, and P. Roentgens, "Local mirror temperatures of red-emitting (Al)GaInP quantum-well laser diodes by Raman scattering and reflectance modulation measurements," *Appl. Phys. Lett.*, vol. 60, no. 6, pp. 680–682, Feb. 10, 1992.

[6] P. W. Epperlein, P. Buckmann, and A. Jakubowicz, "Lattice disorder, facet heating and catastrophic optical mirror damage of AlGaAs quantum-well lasers," *Appl. Phys. Lett.*, vol. 62, no. 5, pp. 455–457, Feb. 1, 1993.

[7] D. C. Hall, L. Goldberg, and D. Mehuys, "Technique for lateral temperature profiling in optoelectronic devices using a photoluminescence microprobe," *Appl. Phys. Lett.*, vol. 61, no. 4, pp. 384–386, July 27, 1992.

[8] 150 Beta Drive15 238-2932"Algor is a product of Algor, Inc.,", Pittsburgh, PA, USA.

[9] S. Adachi, "Thermal conductivity of InGaAs," in *Properties of Lattice-Matched and Strained Indium Gallium Arsenide*, P. Bhattacharya, Ed: INSPEC (IEEE), 1991, pp. 35–40.

[10] J. C. Brice, "Thermal conductivity of indium phosphide," *Properties of Indium Phosphide: EMIS Data Series 6*, pp. 20–21, 1991.

[11] S. Adachi, "Chapter 4: Thermal properties," in *Physical Properties of III–V Semiconductor Compounds: InP, InAs, GaAs, GaP, InGaAs, InGaAsP*. New York: Wiley Interscience , 1992, pp. 55–62.

[12] ——, "Lattice thermal resistivity of III–V compounds," *J. Appl. Phys.*, vol. 54, no. 4, pp. 1844–1848, Apr. 1983.

[13] Y. S. Touloukian, R. W. Powell, C. Y. Ho, and P. G. Clemens, "Thermophysical properties of matter: Thermal conductivity, nonmetallic solids," in *The TPRC Data Series*. New York: IFI/Plenum, 1970, vol. 2.

[14] H. S. Carslaw and J. C. Jaeger, *Conduction of Heat in Solids*, 2nd ed. Oxford, U.K.: Oxford, 1959, pp. 10–11.

[15] A. Goel and A. Gray, "Liquid crystal technique as a failure analysis tool," in *Proc. IEEE Int. Reliability Phys. Symp.*, 1981, p. 115.

[16] J. Hiatt, "A method of detecting hot spots using liquid crystals," in *Proc. IEEE Int. Reliability Phys. Symp.*, 1981, pp. 130–133.

M. Allard, photograph and biography not available at the time of publication.

R. A. Masut, photograph and biography not available at the time of publication.

M. Boudreau, photograph and biography not available at the time of publication.